Active Targeting of Orthotopic Glioma Using Biomimetic Liposomes Co-loaded Elemene and Cabazitaxel Modified By Transferritin

JIE LI
Chengdu University of TCM: Chengdu University of Traditional Chinese Medicine
Huamin Zeng
chengdu pingan healthcare medical examination laboratory
Yu You
Chengdu University of Traditional Chinese Medicine Wenjiang Campus: Chengdu University of Traditional Chinese Medicine
Rongrong Wang
Hangzhou Normal University
Tiantian Tan
Hangzhou Normal University
Weiming Wang
Hangzhou Normal University
Liyan Yin
Hangzhou Normal University
Zhaowu Zeng
Hangzhou Normal University
Yiying Zeng
Hangzhou Normal University
Tian Xie (hznu_xie@126.com)
Hangzhou Normal University

Research Article

Keywords: Glioma, Biomimetic liposomes, Homologous-targeting, Immune escaping, Blood-brain barrier, Transferrin

Posted Date: July 21st, 2021

DOI: https://doi.org/10.21203/rs.3.rs-717860/v1

Abstract

Efficient chemotherapy for glioma demands a nanocarrier that can overcome the blood-brain barrier (BBB) and then target the tumor location. Elemene (ELE) and cabazitaxel (CTX) liposomes are prepared by conjugating liposomes with transferrin (Tf) and embedding the cell membrane proteins of RG2 glioma into liposomes (active-targeting biomimetic liposomes, Tf-ELE/CTX@BLIP), which are demonstrated resultful in infiltrating the BBB and targeting glioma, respectively. Tf-ELE/CTX@BLIP is highly stable, displaying a prominent peculiarity of homologous targeting and of immune evasion *in vitro*, and a 5.83-fold intake rate when versus classical liposome (ELE/CTX@LIP). The result of bioluminescence imaging revealed enhanced drugs accumulation in the brain and increased tumor penetration of Tf-ELE/CTX@BLIP in orthotopic glioma model nude mice. *In vivo* studies demonstrated that the anti-tumor effect of the Tf-ELE/CTX@BLIP include increased survival time and decreased tumor volume. Following intravenous administration of Tf-ELE/CTX@BLIP, the tumor averaged fluorescence intensity was 65.2, 12.5, 22.1, 6.6, 2.6, 1.5 times weaker than that of the control, CTX solution, ELE solution, ELE/CTX@LIP, ELE/CTX@BLIP, Tf-ELE/CTX@LIP groups, respectively. Moreover, histopathological analyses demonstrated that Tf-ELE/CTX@BLIP were less toxic than the CTX solution. These results suggest that the active-targeting biomimetic liposomes, Tf-ELE/CTX@BLIP, is a promising nanoplatform for glioma chemotherapy.

Introduction

Glioma is one of the most threatening disease to human with a high incidence and mortality rate in central nervous system tumors [1, 2]. Up to now, chemotherapy is the most immediate and effective anticancer strategies for glioma due to the characteristic of heterogeneity, invasion and inability to be completely resected by surgical resection [3, 4]. Chemotherapy in glioma, however, is usually hampered by selective penetrability of the blood-brain barrier (BBB), central nervous system toxicity and low targeting of drugs into the tumor site [5-9]. Especially, there is an ATP-dependent efflux pump P-glycoprotein (*P-gp*) on BBB, which increase the clearance of chemotherapy drugs [10]. Therefore, it is essential to design a vehicle that can penetrate BBB, escape efflux mechanism, target into glioma and not cause neurotoxicity.

Liposomes are cell-like spherical vesicles formed by phospholipids and cholesterol that have attracted wide interest in biocompatibility and crossing the BBB abilities [11]. Nevertheless, the lack of active targeting and tumor targeting abilities greatly hampers their applications to glioma chemotherapy. Interestingly, there are kinds of receptors overexpressed on BBB, like insulin receptors, transferrin receptors, endothelial growth factors receptors and amino acids receptors [12]. Receptor-mediated endocytosis is the main pathway for chemotherapeutic agents to enter the brain through the BBB [13, 14]. Here, a targeting ligand—transferrin (Tf) was used to modify liposome for increasing BBB penetrating efficiency by specifically recognizing with transferrin receptors [15]. Although chemotherapeutic agents accumulation in the brain could be enhanced through the above approach, targeting glioma site remains challenging.

To further augment the chemotherapeutic agents accumulation in glioma location, active-targeting biomimetic liposomes were developed by embedding Tf-liposomes with glioma cell membrane proteins (CMP). Near term, CMP-based biomimetic nanoengineering obtained much focus and was subsequently applied in the research of biomimetic liposomes [16-18]. Due to specific homologous recognition to the CMP of source cancer cell, the immune system cannot recognize CMP-camouflaged liposomes. Therefore, the biomimetic liposomes have obtained remarkable peculiarity of targeting and immune escape [19, 20]. The CMP-based biomimetic nanoengineering has been widely applied on biomedical field, such as immunotherapy, bioimaging, theranostics and glioma phototheranostics since the first report in 2014 [18, 21-23]. However, active-targeting biomimetic liposomes of drug co-delivery for glioma chemotherapy are rarely reported, to the best of our knowledge.

Drugs combination is also another important factor in the successful treatment of gliomas [24, 25]. Studies had shown that cabazitaxel (CTX) can inhibit the proliferation of cancer cells by binding to tubulin [26]. In addition, CTX is also the substrate of *P-gp*, which is low affinity to *P-gp* and is not easy to cause drug resistance [27, 28]. CTX has obvious inhibitory effect on glioma, however, it is more toxic [29]. Elemene (ELE), the fat-soluble small molecular compound, can pass through the BBB and owns a definite effect on malignant gliomas in clinical application [30-32]. According to the previous found of author's teams that ELE and CTX (preferably 5:1 weight ratio) encapsulated in the same nanoparticles had a synergistic effect and reduced toxicity [33]. The same effect could be achieved when the dosage of nanoparticles was only 25% of the conventional CTX injection. Therefore, the co-embedding of ELE and CTX in nanoparticles is expected to achieve the best antiglioma effect.

Herein, we produced ELE and CTX liposomes by conjugating liposomes with Tf and embedding CMP into liposomes (Tf-ELE/CTX@BLIP) for permeating BBB and homotypic targeting chemotherapy of orthotopic glioma-bearing mice (**Fig. 1**). The ability of Tf-ELE/CTX@BLIP in *P-gp* inhibition, active targeting, immune escape, cytotoxicity assay and apoptosis promotion *in vitro* and distribution *in vivo* was studied. Meanwhile, the anti-glioma efficacy and biosecurity of Tf-ELE/CTX@BLIP were assessed on orthotopic glioma-bearing mice, too.

Materials And Methods

Materials

ELE was purchased from Dalian Huali Jingang Pharmaceutical Co. LTD (Dalian, China). CTX was purchased from Hubei Qianmo biological technology Co. LTD (Hubei, China). Soybean lecithin was purchased from Shanghai Taiwei pharmaceutical Co. LTD (Shanghai, China). D-α-tocopherol polyethylene glycol succinate (TPGS) was purchased from Wuhan Guobangda pharmaceutical chemical Co. LTD (Wuhan, China). Medium chain triglyceride (MCT) was purchased from Xinxing Tieling pharmaceutical Co. LTD (Tieling, China). Cholesterol (Chol) were purchased from Beijing Dingguo Changsheng Biotechnology Co. LTD (Beijing, China). DSPE-PEG2000-transferrin were purchased from Xi 'an Ruixi Biological Technology Co. LTD (Xi 'an, China). DAPI and GAPDH were purchased from Sigma-Aldrich (St Louis, USA). Penicillin-streptomycin and high-glucose DMEM, trypsin EDTA and FBS were purchased from Gibco Life Technologies (AG, USA). CCK-8 was purchased from Meilunbio (Dalian, China). Cypate were purchased from Hangzhou Xinqiao Biotechnology Co. LTD (Hangzhou, China). Coomassie blue, RIPA lysis buffer and bicinchoninic acid protein kit (BCA) were purchased from Biosharp (Shanghai, China). Apoptosis detection kit was purchased from Genview (USA).

Cell Culture

SPC-A-1 (human lung adenocarcinoma cell), A549 (lung cancer cell), MDA-MB-231 (human breast cancer cell), LM-3 (liver cancer cell), U251 glioma cells, C6 glioma cells, and RG2 glioma cells were cultured in high-glucose (4.5 g/L) DMEM containing 10% FBS, 1% penicillin-streptomycin, 110 mg/L Sodium Pyruvate, and 2 mM L-glutamine and were incubated in normoxic conditions (5% CO_2, 37 °C).

Isolation of CMP

CMP were extracted from RG2 glioma cells as reported in the literature with little adjustment [18, 34, 35]. Briefly, RG2 cells were harvested and resuspended in 4 ℃ Tris-magnesium buffer (TM-buffer, pH 7.4) for 30 min, and crushed 5 min by ultrasonic cell pulverizer (Xinyi-950E, 238W, 2s on, 3s off). 1 mL 1 M sucrose solution was mixed with 3 mL cell debris and the mixed homogenate was centrifuged to discard intracellular contents (2,000 ×g, 10 min, 4 ℃). Whereafter, the CMP were collected by further centrifugation (15,000 ×g, 30 min, 4 ℃) of the supernatant. The CMP were washed with pre-cooled TM-buffer (pH 7.4) containing 0.25 M sucrose, and subsequently gathered by centrifugation (15,000 ×g, 30 min, 4 ℃). Finally, the CMP were resuspended in PBS (1×) and attrition crushing through 0.45 μm pores, determined by BCA protein assay for further preparation of liposomes. The CMP from 3×10^8 cells were 0.76 mg and stored at -20 ℃.

Preparation and Characterization of Tf-ELE/CTX@BLIP

There were four types of liposomes, ELE/CTX@LIP, Tf-ELE/CTX@LIP (ELE/CTX@LIP modified with Tf), ELE/CTX@BLIP (ELE/CTX@LIP modified with CMP), Tf-ELE/CTX@BLIP (ELE/CTX@LIP modified with both Tf and CMP). The synthetic process of active-targeting biomimetic liposomes was presented in **Fig. 1A** ELE/CTX@LIP and Tf-ELE/CTX@LIP were prepared by high speed shear method combined with probe ultrasonic method [33, 36]. In brief, Tf-ELE/CTX@LIP: (I) 8 mg CTX was dissolved in 0.25 mL ethanol by ultrasound. Then, 80 mg ELE, 20 mg cholesterol, 500 mg soybean lecithin, 100 mg TPGS, 10 mg DSPE-PEG2000-transferrin and 100 mg MCT were added. The mixture was heated and dissolved in 80 ℃ water bath as the oil phase. (II) 520 mg glycerol was dissolved in 18.5 g water, kept shear at 3000 rpm at 60 ℃, as the aqueous phase. (III) The oil phase was slowly injected into the aqueous phase, and the shear was performed under the condition of 60 ℃ and 10000 rpm for 30 min (IKA® T25 Easy Clean Digital Dispersion Machine, Germany), and then the particle size was reduced by probe ultrasound for 10 min (Xinyi-950E ultrasonic cell pulverizer, China). ELE/CTX@LIP was prepared by the same process without adding DSPE-PEG2000-transferrin. The CMP-based liposomes were produced by a direct extrusion approach. Tf-ELE/CTX@BLIP was manufactured based on Tf-ELE/CTX@LIP, and ELE/CTX@BLIP was based on ELE/CTX@LIP. Briefly, CMP were mixed with the Tf-ELE/CTX@LIP or ELE/CTX@LIP at 100:1 phospholipid to CMP weight

ratio [18]. Afterward, the mixture was direct extruded through 0.45 μm and 0.22 μm pores to develop Tf-ELE/CTX@BLIP and ELE/CTX@BLIP.

The morphology of 4 types of liposomes was characterized by transmission electron microscope (TEM, HITACHI HT7700 Exalens, Japan). The size distribution and ζ-potential of liposomes were determined by dynamic light scattering measurement (DLS, PSS Nicomp 380 Z3000 Zeta Potential and Nano particle Size meter, PSS, USA). The storage stability and serum stability of Tf-ELE/CTX@BLIP in water, PBS and PBS containing 10% FBS were analyzed by the diameter change over 7 days using DLS. CMP and Tf-ELE/CTX@BLIP protein profiles were detected by sodium dodecyl sulfate polyacrylamide gel electrophoresis (SDS-PAGE), and the protein marker GAPDH and (ATP1A1, ATPase) was analyzed by western blot (WB). The encapsulation efficiency (EE) and drug loading efficiency (DLE) of ELE and CTX were determined by HPLC (1260 Infinity II High Performance Liquid chromatograph, Agilent Technologies, USA) according to the following chromatographic conditions and measured according to the equation of EE= (W_a/W_a+W_b) ×100% and DL= $[W_a/W_t)]$ ×100%, where W_a represented the amount of ELE or CTX encapsulated in liposomes after hyperfiltration, Wb represented the amount of ELE or CTX unencapsulated, and W_t represented the total amount of phospholipid.

ELE: Ultimata PAH chromatographic column (300 x 4.6 mm, 3 μm). Mobile phase A: 75% acetonitrile-25% 0.01% phosphoric acid water; Mobile phase B: 0.01 % acetonitrile phosphate. Elution conditions: 0~45 min, 80% A+20% B, 45.01~65 min, 100% B. The flow rate: 1.2 mL/min, the injection volume: 20 μL, the column temperature: 40 ℃ and the detection wavelength: 210 nm.

CTX: Agilent PFP chromatographic column (250×4.6 mm, 5 μm). Mobile phase A: 51 % acetonitrile-49% 0.01% phosphoric acid water; Mobile phase B: 0.01 % acetonitrile phosphate. Elution conditions: 0~25 min, 100 %, 25.01~45 min, 100 % B. The flow rate: 1.0 mL/min, the injection volume: 20 μL, the column temperature: 30 ℃ and the detection wavelength: 230 nm.

In Vitro Cancer Targeting Study and Cell Uptake

Tf-ELE/CTX@BLIP was incubated with SPC-A-1 cells, A549 cells, MDA-MB-231 cells, LM-3 cells, U251 cells, C6 cells, and RG2 cells, respectively. Briefly, cells were inoculated into 6-well plates (3×10^5 cells/well) for 24 h. After incubation, anterior medium was removed and replaced by fresh medium containing Tf-ELE/CTX@BLIP (Rhodamine B [Rho B] = 20 μg/mL) for 2 h. In addition, RG2 cells in 6-well plate (3×10^5 cells/well) were also incubated with ELE/CTX@LIP, ELE/CTX@BLIP, Tf-ELE/CTX@LIP and Tf-ELE/CTX@BLIP (Rho B = 20 μg/mL) for 2 h. After removing the medium, cells was fixed with 4% paraformaldehyde, stained with DAPI, washed with PBS thrice, and finally the cellular uptake was measured by confocal laser scanning microscope imaging (CLSM, FV3000RS, OLYMPUS, USA) and flow cytometry [37].

Macrophage RAW264.7 cells were exposed to ELE/CTX@LIP, ELE/CTX@BLIP, Tf-ELE/CTX@LIP and Tf-ELE/CTX@BLIP (Rho B = 20 μg/mL) for 2 h, and the peculiarity of immune evasion was calculated by CLSM and flow cytometry [38].

In Vitro Cytotoxicity Assay and Cell Apoptosis

The cytotoxicities of ELE/CTX@LIP, ELE/CTX@BLIP, Tf-ELE/CTX@LIP and Tf-ELE/CTX@BLIP were determined in RG2 cells by CCK-8 kit. In brief, RG2 cells (3,000 cells/well) were inoculated in 96-well plates for 24 h. After incubation, cells were exposed to ELE/CTX@LIP, ELE/CTX@BLIP, Tf-ELE/CTX@LIP and Tf-ELE/CTX@BLIP (CTX concentrations ranging from 0.4 to 200 ng/mL) for 48 h. The non-treated cells acted as negative controls. By contrast, medium was evaluated as the blank control. The cytotoxicity was quantitatively determined by measuring the absorbance at 450 nm with Spark multi-functional microporous plate testing platform (Tecan, Switzerland).

Furthermore, the apoptotic cells were counted by FACS analysis (CytoFLEX S, USA). RG2 were incubated with ELE/CTX@LIP, ELE/CTX@BLIP, Tf-ELE/CTX@LIP and Tf-ELE/CTX@BLIP at 50 ng/mL of CTX for 48 h and then treated with the apoptosis detection kit (Genview, USA) for 10 min. Subsequently, the percentage of apoptotic cells was analyzed by the FACS Calibur System. Non-treated cells performed as the negative control [39].

Inhibitory Effect of Tf-liposomes on P-gp Function

bEnd.3 cell were cultured in accordance with *"2.2.1.Cell culture"*. In brief, cells were inoculated into 6-well plates (5×10^5 cells/well) for 24 h. Preconditioned with ELE/CTX@LIP, ELE/CTX@BLIP, Tf-ELE/CTX@LIP, Tf-ELE/CTX@BLIP (50 ng/mL) and verapamil (0.625 μg/ mL) for 30 min respectively, rhodamine 123 (*P-gp* substrate, 20 μg/ mL) was exposed to bEnd.3 for 2 h. After removing medium, bEnd.3

cells was fixed with 4% paraformaldehyde for 30 min, washed with PBS thrice, and finally measured using fluorescence microscope and flow cytometry [40].

Animal and Orthotopic Glioma-bearing Model

Female nude mice (20±2 g, BALB/c) were obtained from Shanghai Slack Laboratory Animal Co. LTD. The study was performed after the mice were allowed to acclimate at room temperature and allowed free access to food/water under the animal care facility for 7 days. All animal experiments were performed with permission by the animal ethics committee of Hangzhou Normal University (HangZhou, China).

Glioma-luc cells were injected into the right striatum of nude mouse to develop a orthotopic glioma-bearing model. In brief, nude mouse was anesthetized with 10% chloral hydrate and the head was immobilized on a stoelting (Lab Standard, USA). Afterwards, approximately 2.5×10^7 glioma-luc cells in medium were injected into the brain right striatum of nude mouse (bright lateral: 2.0 mm, bregma: 1.8 mm, depth: 3.5 mm). The cells are injected slowly. Stay for 1 minute after injection and pull out the needle slowly. Alcohol cotton swabs disinfect the skin, sew up the skin with needle and thread, and then put the mice back into the cage to wake up naturally. The growth situation of intracranial tumor was monitored by magnetic resonance imaging (MRI) and fluorescence imaging .

In Vivo Bioluminescence Imaging

A orthotopic glioma-bearing model was established by injecting RG2 cells into the brain striatum according to the above method. Free Cypate, Cypate@LIP, Cypate@BLIP, Tf-Cypate@LIP and Tf-Cypate@BLIP (C_{Cypate}= 0.1 mg/mL) was injected into normal mice and glioma-bearing mice *via* tail vein, and bioluminescence images were performed at fixed times (2, 8, 24 and 48 h) through a small animals *in vivo* 3D bioluminescence imaging system (IVIS Spectrum, PerkinElmer). Subsequently, nude mice were sacrificed, and brains, liver, heart, spleen, lung, and kidney were collected for quantitative biodistribution analysis and *ex vivo* bioluminescence imaging [41].

In Vivo Anti-tumor Study

Orthotopic glioma-bearing model nude mice were randomly divided into seven groups (6 mice/group): (1) control (physiological saline); (2) CTX solution; (3) ELE solution (25 mg/kg ELE); (4) ELE/CTX@LIP; (5) ELE/CTX@BLIP; (6) Tf-ELE/CTX@LIP; (7) Tf-ELE/CTX@BLIP, to evaluate the anti-tumor effect *in vivo*. The drug was administered by tail intravenous injection at days 1, 3, 5, 7, 9 and 11. Group 2, 4, 5, 6, 7 was given 2.5 mg/kg (CTX) for the first time and 0.625 mg/kg for the next 5 times. Bioluminescence imaging were performed at days 1, 5, 10, and 15 to represent tumor growth. The body weight every 3 days and survival time were recorded. At 2 h post-treatment, nude mice were euthanized and their brains were collected for H&E staining, TUNEL immunofluorescence staining and detection of glioma *P-gp*.

Toxicity Evaluation

Glioma-bearing nude mice were divided into 7 groups and were injected with (1) control (physiological saline); (2) CTX solution; (3) ELE solution; (4) ELE/CTX@LIP; (5) ELE/CTX@BLIP; (6) Tf-ELE/CTX@LIP; (7) Tf-ELE/CTX@BLIP, respectively, 6 times every other day. At 2 h post-treatment, whole blood samples were collected from retro-orbital sinus of glioma-bearing nude mice. A part of complete blood samples were used for complete blood count analysis. The supernatant (serum) of another part of blood after centrifugation (5,000 rpm, 10 min) was taken to detect the biochemical indexes of liver and kidney, including total bilirubin, blood urea nitrogen, uric acid, alanine transaminase, creatinine and aspartate transaminase. Liver, heart, spleen, lung and kidney section stained with H&E to evaluate the free ELE, CTX solution and liposomes toxicity [42].

Statistical Analysis

GraphPad Prism 8.0.2.263 software (GraphPad Software Inc., San Diego, CA, USA) was used for statistical analysis. Results data were expressed as mean ± SD. The experimental data were analyzed using two-tailed Student *t* test for different groups. Statistical difference was defined as significant for $*p < 0.05$ and very significant for $**p < 0.01$.

Results And Discussion

Preparation and Characterization of Tf-ELE/CTX@BLIP

The 4 liposome samples, which were opalescent translucent liquids and their particle sizes had illustrated in **Fig. 2A, 2B** The mean particle sizes, PI, ζ-potentials, EE and DLE of different formulations were listed in **Table 1** and **Fig. S1** Particle sizes of liposomes with CMP (Tf-ELE/CTX@BLIP: size 135.1±4.2 nm, PDI=0.263 and ELE/CTX@BLIP: size 115.7±1.3 nm, PDI=0.168) were slightly bigger than liposomes without CMP (Tf-ELE/CTX@LIP size 153.0±3.4 nm, PDI=0.345 and ELE/CTX@LIP size 135.4±2.0 nm, PDI=0.205), demonstrating that the CMP embed into the lipid bilayer by continuous extrusion. The EE of ELE/CTX were determined to be 99.827±0.004% and 99.106±0.378% in the Tf-ELE/CTX@BLIP, respectively. The ζ-potential was 33.57±0.67 mV. As shown in **Fig. 2C**, TEM imaging of 4 types of liposomes indicated that the liposome owned spherical nanostructures. Simultaneously, when compared to liposomes without CMP (ELE/CTX@LIP and Tf-ELE/CTX@LIP), ELE/CTX@BLIP and Tf-ELE/CTX@BLIP appeared an irregular spherical shape for inseting of CMP. Whereafter, SDS-PAGE and WB were implemented to verify the protein profile of ELE/CTX@BLIP and Tf-ELE/CTX@BLIP. As shown in **Fig. 2D, 2E**, the protein profile of Tf-ELE/CTX@BLIP was consistent with RG2 cells and CMP. In addition, WB analysis demonstrated the presence of ATP1A1 (a membrane-specific marker) on Tf-ELE/CTX@BLIP, declaring that CMP were successfully embed onto the surface of Tf-ELE/CTX@BLIP. As shown in **Fig. 2F, 2G**, no significant particle size changes were detected after 7 days of storage in 4 ℃, suggesting a excellent storage stability of Tf-ELE/CTX@BLIP, as well as ζ-poteneial. Further, no obvious size changes of Tf-ELE/CTX@BLIP were monitored within 7 days in PBS (pH 7.4) and PBS containing 10 % FBS (**Fig. S2**), demonstrating the good serum stability of the Tf-ELE/CTX@BLIP is appropriate for potential application and study *in vitro/vivo*.

Table 1 Characteristics of liposomes (n = 3).

Samples	Size/nm	PDI	ζ-poteneial/mV	EE (%)		DLE (%)	
				ELE	CTX	ELE	CTX
Tf-ELE/CTX@BLIP	135.1±4.2	0.263±0.018	33.57±0.67	99.827±0.004	99.106±0.378	16.376±0.001	1.640±0.006
Tf-ELE/CTX@LIP	153.0±3.4	0.345±0.011	54.96±1.91	99.296±0.397	99.419±0.104	16.113±0.064	1.609±0.002
ELE/CTX@BLIP	115.7±1.3	0.168±0.023	33.95±1.08	99.767±0.001	97.175±0.013	15.963±0.001	1.555±0.0002
ELE/CTX@LIP	135.4±2.0	0.205±0.021	34.53±2.66	97.701±0.397	95.640±0.218	15.826±0.064	1.545±0.004
CMP	-	-	30.12±0.73	-	-	-	-

Homologous Targeting and Immune Escape Abilities of Tf-ELE/CTX@BLIP

To evaluate the specific homologous targeting abilities of Tf-ELE/CTX@BLIP by homotypic cancer cells, the cellular uptake of several different cell lines by Tf-ELE/CTX@BLIP was evaluated, including RG2, APC-A-1, C6, U87, LM-3 and MBA-MD-231. According to the results, the fluorescence intensity of Tf-ELE/CTX@BLIP in the RG2 cell group was 1.21- to 2.02-fold stronger than other cell lines (**Fig. 3A, 3B**), demonstrating Tf-ELE/CTX@BLIP achieved higher uptake efficiency to RG2 cells and further confirming the homologous adhesion property induced prominent active targeting characters.

In addition, the uptake of Tf-ELE/CTX@BLIP in RG2 cells was evaluated by CLSM. When compared to the other treated groups, a higher amount of Tf-ELE/CTX@BLIP were ingested into the RG2 cells cytoplasm, after incubation at 37 ℃ for 2 h with ELE/CTX@LIP, Tf-ELE/CTX@LIP, ELE/CTX@BLIP and Tf-ELE/CTX@BLIP, respectively (**Fig. 3C**), further suggesting that Tf-ELE/CTX@BLIP acquired homologous targeting ability for the stronger fluorescence signal. The quantitative analysis results by flow cytometry showed the fluorescence intensity in Tf-ELE/CTX@BLIP-treated cells was 3.34- to 5.83-fold stronger than that other gropes (**Fig. 3D, S3)**, revealing its excellent active targeting ability. Compared with C6 and U251, the uptake efficiency of TF-ELE /CTX@BLIP in RG2 was significantly increased **(Fig. S4**).

Moreover, the internalization of Tf-ELE/CTX@BLIP, Tf-ELE/CTX@LIP, ELE/CTX@BLIP and ELE/CTX@LIP by RAW264.7 macrophages was detected by flow cytometry and CLSM imaging to test the antiphagocytic properties. As shown in **Fig. 3E, 3F, S5**, just a little of Tf-ELE/CTX@BLIP and ELE/CTX@BLIP were internalized by RAW 264.7 macrophages, which exhibited 1.83- and 1.92-fold weaker fluorescence intensity than that of Tf-ELE/CTX@LIP and ELE/CTX@LIP treated cells, indicating the excellent immune escape characteristics of biomimetic liposomes. Of note, the phagocytosis of RAW 264.7 macrophages may be enhanced for the addition of Tf.

In Vitro Cytotoxicity Assay and Cell Apoptosis of Tf-ELE/CTX@BLIP

The results of CCK-8 quantitative analysis disclosed that the IC50 of ELE/CTX@LIP, ELE/CTX@BLIP, Tf-ELE/CTX@LIP and Tf-ELE/CTX@BLIP (C_{CTX} 0.4 to 200 ng/mL) group was 27.38±0.67, 31.30±1.44, 42.70±0.76 and 54.25±4.90 ng/mL, respectively (**Fig. 4A**), suggesting a much higher against glioma cells effect of Tf-ELE/CTX@BLIP. Meanwhile, the cell inhibition ratio in the Tf-ELE/CTX@BLIP, Tf-ELE/CTX@LIP, ELE/CTX@BLIP and ELE/CTX@LIP (C_{CTX} = 50 ng/mL) was 56.50±0.86%, 54.69±1.79%, 52.41±1.50% and 49.44±1.33%, respectively (**Fig. 4B, 4C**). The higher cytotoxicity induced by Tf-ELE/CTX@BLIP in RG2 cells indicated the promising superiorities for *in vivo* research and applications.

A dual staining assay was executed by flow cytometry to quantitatively analyze apoptotic cells. A significant increase of the apoptosis number was monitored in RG2 cells when incubated with Tf-ELE/CTX@BLIP (60.97%), ELE/CTX@BLIP (56.02%), Tf-ELE/CTX@LIP (60.80%) and ELE/CTX@LIP (42.49%), compared to the control group (25.68%), CTX solution group (42.47%) and ELE+CTX solution group (67.89%) (**Fig. 4D**), demonstrating that ELE+CTX inhibits the proliferation of glioma cells by activating apoptosis channel, and Tf-ELE/CTX@BLIP enhances the effect of promoting apoptosis by conjugating liposomes with Tf and embedding CMP into liposomes, which was agreed with the cytotoxicity assay.

Inhibitory Effect of Tf-liposomes on P-gp Function

The accumulation of Rho 123 in bEnd.3 cell incubated with Tf-ELE/CTX@BLIP, Tf-ELE/CTX@LIP, ELE/CTX@BLIP and ELE/CTX@LIP was detected to monitor the transportation of different formulations across BBB. *P-gp* is one of the main physiological disorders on the BBB (the efflux effect). With verapamil (a *P-gp* efflux inhibitor) as a positive control, the fluorescent substrate Rho 123 of *P-gp* can be used to study the efflux effect. The results suggested that the efflux of Rho 123 from the bEnd.3 cells after incubating with Tf-ELE/CTX@LIP and Tf-ELE/CTX@BLIP was significantly reduced than the control group, demonstrating Tf-ELE/CTX@BLIP and Tf-ELE/CTX@LIP could greatly improve the penetrability of Rho 123 through BBB (**Fig. 4E**). Similar results were achieved by flow cytometry, implying that the fluorescence intensity in Tf-ELE/CTX@BLIP and Tf-ELE/CTX@LIP-treated cells was increased obviously (**Fig. 4F**), revealing the suppressed efflux effect.

In Vivo Homologous Targeting Bioluminescence Imaging

In order to further assess the active targeting ability of liposome modified with CMP/Tf and study the distribution *in vivo*, we implanted glioma cells into the striatum of mice and established an orthotopic glioma model. Fluorescence imaging was used to appraise the glioma-luc cells activity. MRI showed the glioma area of nude mice after 15 days of glioma cell implantation (**Fig. 5A, 5B**). Glioma cells owned excellent proliferation activity, proving by the forceful fluorescence signal of the tumor (**Fig. 5C**). In addition, Tf-Cypate@BLIP, Tf-Cypate@LIP, Cypate@BLIP, Cypate@LIP and free Cypate was injected into normal mice and orthotopic glioma mice *via* tail vein. In the brains of mice treated with free Cypate, no bioluminescence signal was monitored (**Fig. 5D, 5E**). And averaged intensity of Tf-Cypate@BLIP, Tf-Cypate@LIP, Cypate@BLIP, Cypate@LIP group have no obvious different, indicating that the early stage of tumor was dominated by the enhanced permeability and retention effect. However, Tf-Cypate@BLIP and Cypate@BLIP with excellent peculiarity of homologous targeting and of immune evasion was capable to permeate easily the BBB and specifically recognize to the homologous cells. Moreover, Tf can also inhibit the efflux of *P-gp*, allowing more drugs to accumulate in the brain for longer (**Fig. 5D**). The *ex vivo* bioluminescence images implied the liposomes were mainly distributed in glioma region and liver, and slightly distributed in kidney (**Fig. 5F, S6**), demonstrating the distinguished tumor targeting and potential hepatic and renal metabolic pathways of the liposomes, which was accorded with the results of quantitative analysis. Furthermore, the strongest fluorescent signal also prove that Tf-ELE/CTX@BLIP is superior to infiltrate the damaged BBB and arrive the glioma region than other liposomes (**Fig. S6**). However, the accumulation of liposomes in liver and kidney may cause hepatorenal toxicity, so further experiments are needed to evaluate the safety. Similarly, numerous fluorescent signal in the orthotopic glioma-bearing mice brain was detected, whereas only few liposome was absorbed by brain tissue of normal mice, and enriched for a shorter time (**Fig. 5G, S7)**, demonstrating that glioma cells entered the brain and grew rapidly causing damage to the local BBB. And liposome does not enter normal brain tissue, except for glioma cells, which in accordance with the result of the significantly higher expression of Tf receptor in the capillary endothelial cells of tumor-bearing mice brain than that of normal mice brain tissue.

In Vivo Anti-tumor Efficacy of Tf-ELE/CTX@BLIP

Fluorescence imaging was implemented to visualize the anti-glioma effect *in vivo*. As illustrated in **Fig. 6A**, fluorescence signal in brain tumor of orthotopic glioma-bearing mice exposed to Tf-ELE/CTX@BLIP was obvious lower than other groups after 15 days treatment. Quantitative analysis and tumor fluorescent intensity showed a tumor growth suppressing effect by Tf-ELE/CTX@BLIP, the tumor averaged fluorescence intensity was 65.2, 12.5, 22.1, 6.6, 2.6, 1.5 times weaker than that of the control, CTX solution, ELE

solution, ELE/CTX@LIP, ELE/CTX@BLIP, Tf-ELE/CTX@LIP groups, respectively. (**Fig. 6B, 6C, S8**). Indeed, Tf-ELE/CTX@BLIP group displayed lowest tumor fluorescence signal than other groups after 15 day administration. The results were coincided with the fluorescence signal, suggesting that Tf-ELE/CTX@BLIP-mediated chemotherapy could inhibit glioma growth significantly. Based on the above experiments, the anti-glioma effect of Tf-ELE/CTX@BLIP was further manifested by median survival time (MST) and body weight (**Table 2, Fig. 6D, 6E**). Obviously, body weights of control, ELE solution groups were dropped sharply from the 9th day of treatment, however, that of CTX solution, ELE/CTX@LIP, ELE/CTX@BLIP, Tf-ELE/CTX@LIP and Tf-ELE/CTX@BLIP groups displayed continuous increase within 15 days of administration, implying that excellent anti-tumor efficacy of drug-loaded liposomes was beneficial to improve physical condition. The MST of ELE/CTX@LIP group's was 28 days, demonstrating the advanced anti-glioma efficiency than the control, CTX solution and ELE solution groups. The ELE/CTX@BLIP and Tf-ELE/CTX@LIP groups' MST was 31 and 30 days, respectively, illustrating that the MST was improved than that of CTX solution and traditional liposome. The result demonstrated that targeting liposome owned better antiglioma effectiveness. The MST of the Tf-ELE/CTX@BLIP group was 33 days, advanced by 6.5% and 10.0% than the ELE/CTX@BLIP and Tf-ELE/CTX@LIP groups, suggesting that Tf and CMP contributed together to the anti-glioma efficiency of Tf-ELE/CTX@BLIP, for the drugs brain accumulation and homologous gliomas targeting.

Table 2 Survival time of nude mice bearing orthotopic glioma after treatment (n=3).

Groups	Median (days)	Mean survival (days)	Maximal survival (days)	Incremental survival time (%)	*P* value (vs control)	*P* value (vs CTX solution)
Control	23	23.0±1.7	24	—	—	0.0295
CTX solution	27	26.7±2.1	29	15.94	0.0295	—
ELE solution	26	26.0±2.6	29	13.04	0.096	0.1615
ELE/CTX@LIP	28	28.0±2.6	30	21.74	0.0295	0.3722
ELE/CTX@BLIP	31	30.7±2.1	33	33.33	0.0295	0.0629
Tf-ELE/CTX@LIP	30	30.0±4.0	34	30.43	0.0295	0.1341
Tf-ELE/CTX@BLIP	33	33.0±3.0	36	43.48	0.0295	0.0246

As a non-invasive detecting technology, MRI endowed us to directly observe brain area. Herein, MRI was utilized to assesse tumor progression after 15 days cell inoculation. The results showed that less tumor region was described in the Tf-ELE/CTX@BLIP-treated mice as compared with other groups (**Fig. 7A**). Tf-ELE/CTX@BLIP displayed prominent glioma suppressive effectiveness after 15 days implantation of glioma cells. Briefly, irregular isometric T1 mixed T2 space occupying lesions were observed in the brains of glioma-bearing mice in control group and ELE solution group, surrounded by patchiness and macular edema zones. The adjacent brain tissue was oppressed by the tumor, showing glial hyperplasia and unclear boundaries. The left lateral ventricle was narrowed and the midline was shifted to the left. The brain lesions of CTX solution group mice were similar to those in control group and ELE solution group, but no glial hyperplasia was found. Compared with control group and ELE solution group, the mice in ELE/CTX@LIP group showed the same type of lesion, accompanied by edema around the lesion. The compression of the tumor in the adjacent brain tissue narrowed the left lateral ventricle and shifted the midline to the left. No edema was found around the brain lesions in ELE/CTX@BLIP group and TF-ELE/CTX@LIP group, and the adjacent brain tissue was not oppressed, with a distinct middle line. In the TF-ELE/CTX@BLIP group mice, the boundary and midline were clearly visible, with no edema around the lesion and no compression of the tumor in the adjacent brain tissue, indicating that the invasive growth of tumor cells was significantly inhibited.

To explore the potential anti-tumor mechanism, the brain slices of nude mice bearing orthotopic glioma were assessed. The results of H&E staining for the brain slices from Tf-ELE/CTX@BLIP treated group showed that in the control group, the texture of tumor tissue was tight and there were no obvious apoptotic cells and no central necrotic area. The necrotic area was less than 1/4 of the total area, which was coincided with their shorter MST, as compared with other groups (**Fig. 7B, S9**). Tumor size of the free ELE and CTX solution groups mice was reduced, with a small (ELE solution group) or obvious (CTX solution group) number of apoptotic cells, demonstrating a definite anti-glioma efficiency of ELE and CTX. As compared with the free ELE&CTX groups, glioma size of the ELE/CTX@LIP, ELE/CTX@BLIP and Tf-ELE/CTX@LIP groups mice further reduced. The texture was loose, with obvious apoptotic cells and central

necrotic area. The necrotic area was close to 1/2 of the total area, demonstrating the intensive antiglioma effect. Moreover, the glioma size of Tf-ELE/CTX@BLIP group was the smallest, where the necrosis area was approach to 3/4 of the total tumor area, indicating that the active-targeting biomimetic nanoplatform obtained the best antiglioma effect.

To appraise the apoptosis-inducing ability of Tf-ELE/CTX@BLIP, the brain slices were observed and stained by TUNEL immunofluorescence. The highest apoptosis rate was monitored at the Tf-ELE/CTX@BLIP-treated mice, which was consistent with the cell apoptosis experiment (**Fig. 4D**), indicating that Tf-ELE/CTX@BLIP could accelerate tumor apoptosis *in vivo*, while the apoptotic activity of the control group was negligible (**Fig. 7C**). Furthermore, the *P-gp* expression was also evaluated. The lowest *P-gp* expression in Tf-ELE/CTX@BLIP than the control group, ELE/CTX solution group and classical liposome, suggesting the Tf-ELE/CTX@BLIP could not induce the positive *P-gp* expression and could steer by the efflux effect. (**Fig. 7D**).

In Vivo Biosafety Evaluation of Tf-ELE/CTX@BLIP

To assess the biosafety of Tf-ELE/CTX@BLIP, several blood routine parameters were evaluated. We injected the Tf-ELE/CTX@BLIP, Tf-ELE/CTX@LIP, ELE/CTX@BLIP, ELE/CTX@LIP, ELE solution, CTX solution or physiological saline to nude mice bearing orthotopic glioma *via* tail vein, for their potential clinical reference. Compared to the control group, most of the blood routine parameters of the experimental groups were within the normal physiological reference range (**Fig. 8 A-P**), demonstrating that experimental groups showed no significant hematological toxicity *in vivo*, except platelets of CTX solution. Analogously, the total bilirubin, blood urea nitrogen, uric acid, ALT, creatinine and AST of the Tf-ELE/CTX@BLIP, Tf-ELE/CTX@LIP, ELE/CTX@BLIP, ELE/CTX@LIP, ELE solution were all in the range of control group, indicating that the Tf-ELE/CTX@BLIP displayed no obvious hepatorenal toxicity of mice (**Fig. S10**). As compared with the control group, obvious typical tubular lesion were achieved in kidneys of the CTX solution groups, suggesting a degree of nephrotoxicity of CTX (**Fig. 8 Q**). H&E staining results of liver, heart, spleen, lung and kidney in other groups no obvious or only minor abnormal and inflammatory cell infiltration as compared with control group, indicating that the drugs-combination and liposome could reduced the nephrotoxicity of CTX. Therefore, these experiments proved that the Tf-ELE/CTX@BLIP displayed good biocompatibility to combat glioma.

Conclusion

In summary, liposomes with active-targeting effects, excellent homologous recognition and BBB permeating capacities were prepared for combined chemotherapy of glioma, providing a potential strategy for clinical chemotherapy of glioma. Tf-ELE/CTX@BLIP significantly augment the transfer of ELE/CTX across the BBB and ingesting by glioma. The MST of orthotopic glioma model mice was significantly prolonged and high biosafety was confirmed than CTX solution, displaying an active-targeting biomimetic effectiveness. The findings will promote further research to develop chemotherapy of central nervous system diseases and contribute ideas to the development and research of active-targeting biomimetic nanoparticles.

Declarations

Author contributions

JL, ZZ and TX conceived and designed the experiment. JL, RW, TT, WW and LY carried out the experiment. JL, HZ YY analyzed data and summarized results. JL and HZ drafted the manuscript and drew the figures. ZZ, YZ and TX revised the manuscript.

Funding

This work was supported by the National Natural Science Foundation of China (81730108), Key Project of Zhejiang project Ministry of Science and Technology (Grant No. 2021C03087), Key Project of Hangzhou Ministry of Science and Technology (20212013B03) and the Zhejiang Province Basic public welfare research program of China (Grant No. 1579 LGF20H300006).

Availability of data and materials

All data generated or analyzed during this study are included in this article

Ethics approval and consent to participate

Not applicable for this study.

Consent for publication

We give our consent for the manuscript to be published in Journal of Nanobiotechnology.

Competing interests

The authors declare that they have no competing interests.

Author details

[1] *College of Pharmacy, Chengdu University of Traditional Chinese Medicine, Chengdu, Sichuan, 611137, People's Republic of China.* [2] *College of Pharmacy, School of Medicine, Hangzhou Normal University, Hangzhou, Zhejiang 311121, China.* [3] *Key Laboratory of Elemene Class Anti-Cancer Chinese Medicine of Zhejiang Province, Hangzhou, Zhejiang, 311121, People's Republic of China.* [4] *Engineering Laboratory of Development and Application of Traditional Chinese Medicine from Zhejiang Province, Hangzhou, Zhejiang, 311121, People's Republic of China.* [5] *Chengdu Ping An Healthcare Medical Examination Laboratory, Chengdu, Sichuan, 611130, People's Republic of China.* [6] *Traditional Chinese Medicine College of Guangdong Pharmaceutical University, Guangzhou, 511400, People's Republic of China*

References

1. Bush NA, Chang SM, Berger MS: Current and future strategies for treatment of glioma. Neurosurg Rev 2017, 40:1-14.

2. Gusyatiner O, Hegi ME: Glioma epigenetics: From subclassification to novel treatment options. Semin Cancer Biol 2018, 51:50-58.

3. Li J, Zhao J, Tan T, Liu M, Zeng Z, Zeng Y: Nanoparticle Drug Delivery System for Glioma and Its Efficacy Improvement Strategies: A Comprehensive Review. Int J Nanomedicine 2020, 15:2563-2582.

4. Xu H, Han Y, Zhao G: Hypoxia-Responsive Lipid-Polymer Nanoparticle-Combined Imaging-Guided Surgery and Multitherapy Strategies for Glioma. ACS Appl Mater Interfaces 2020, 12:52319-52328.

5. Braganhol E, Wink MR, Lenz G, Battastini AMO: Purinergic Signaling in Glioma Progression. Adv Exp Med Biol 2020, 1202:87-108.

6. Lu L, Chen H, Wang L, Zhao L, Cheng Y, Wang A: A Dual Receptor Targeting- and BBB Penetrating- Peptide Functionalized Polyethyleneimine Nanocomplex for Secretory Endostatin Gene Delivery to Malignant Glioma. Int J Nanomedicine 2020, 15:8875-8892.

7. Rosca L, Robert-Boire V, Delisle JF, Samson Y, Perreault S: Carboplatin and vincristine neurotoxicity in the treatment of pediatric low-grade gliomas. Pediatr Blood Cancer 2018, 65:e27351.

8. Thakur A, Sidu RK: Inhibition of Glioma Cells' Proliferation by Doxorubicin-Loaded Exosomes via Microfluidics. Int J Nanomedicine 2020, 15:8331-8343.

9. Zhu J, Zhang Y, Chen X, Zhang Y, Zhang K, Zheng H, Wei Y, Zheng H, Zhu J, Wu F, et al: Angiopep-2 modified lipid-coated mesoporous silica nanoparticles for glioma targeting therapy overcoming BBB. Biochem Biophys Res Commun 2021, 534:902-907.

10. Han B, Xie W, Zhang Y, Zhou S, Yang J, Wang R, Sun Y, Wang X, Xu J, Chen D, et al: The influx/efflux mechanisms of d-peptide ligand of nAChRs across the blood-brain barrier and its therapeutic value in treating glioma. J Control Release 2020, 327:384-396.

11. Li J, Tan T, Zhao L, Liu M, You Y, Zeng Y, Chen D, Xie T, Zhang L, Fu C, Zeng Z: Recent Advancements in Liposome-Targeting Strategies for the Treatment of Gliomas: A Systematic Review. ACS Applied Bio Materials 2020, 3:5500-5528.

12. Smith MW, Gumbleton M: Endocytosis at the blood-brain barrier: from basic understanding to drug delivery strategies. J Drug Target 2006, 14:191-214.

13. Ferraris C, Cavalli R: Overcoming the Blood-Brain Barrier: Successes and Challenges in Developing Nanoparticle-Mediated Drug Delivery Systems for the Treatment of Brain Tumours. Int J Nanomedicine 2020, 15:2999-3022.

14. Lu Q, Cai X, Zhang X, Li S, Song Y, Du D, Dutta P, Lin Y: Synthetic Polymer Nanoparticles Functionalized with Different Ligands for Receptor-mediated Transcytosis across Blood-Brain Barrier. ACS Appl Bio Mater 2018, 1:1687-1694.

15. Johnsen KB, Burkhart A, Thomsen LB, Andresen TL, Moos T: Targeting the transferrin receptor for brain drug delivery. Prog Neurobiol 2019, 181:101665.

16. Chai Z, Ran D, Lu L, Zhan C, Ruan H, Hu X, Xie C, Jiang K, Li J, Zhou J, et al: Ligand-Modified Cell Membrane Enables the Targeted Delivery of Drug Nanocrystals to Glioma. ACS Nano 2019, 13:5591-5601.

17. Fu S, Liang M, Wang Y, Cui L, Gao C, Chu X, Liu Q, Feng Y, Gong W, Yang M, et al: Dual-Modified Novel Biomimetic Nanocarriers Improve Targeting and Therapeutic Efficacy in Glioma. ACS Appl Mater Interfaces 2019, 11:1841-1854.

18. Jia Y, Wang X: Phototheranostics: Active Targeting of Orthotopic Glioma Using Biomimetic Proteolipid Nanoparticles. ACS Nano 2019, 13:386-398.

19. Datta B, Paul D, Pal U, Rakshit T: Intriguing Biomedical Applications of Synthetic and Natural Cell-Derived Vesicles: A Comparative Overview. ACS Applied Bio Materials 2021, 4:2863-2885.

20. Mo X, Zheng Z, He Y, Zhong H, Kang X, Shi M, Liu T, Jiao Z, Huang Y: Antiglioma via regulating oxidative stress and remodeling tumor-associated macrophage using lactoferrin-mediated biomimetic codelivery of simvastatin/fenretinide. J Control Release 2018, 287:12-23.

21. Jin J, Bhujwalla ZM: Biomimetic Nanoparticles Camouflaged in Cancer Cell Membranes and Their Applications in Cancer Theranostics. Front Oncol 2019, 9:1560.

22. Fang RH, Hu CM, Luk BT, Gao W, Copp JA, Tai Y, O'Connor DE, Zhang L: Cancer cell membrane-coated nanoparticles for anticancer vaccination and drug delivery. Nano Lett 2014, 14:2181-2188.

23. Zhao P, Wang M, Chen M, Chen Z, Peng X, Zhou F, Song J, Qu J: Programming cell pyroptosis with biomimetic nanoparticles for solid tumor immunotherapy. Biomaterials 2020, 254:120142.

24. Lin GL, Wilson KM: Therapeutic strategies for diffuse midline glioma from high-throughput combination drug screening. Sci Transl Med 2019, 11.

25. Zhao M, van Straten D, Broekman MLD, Préat V, Schiffelers RM: Nanocarrier-based drug combination therapy for glioblastoma. Theranostics 2020, 10:1355-1372.

26. Zhu L, Zhang C, Lü X, Song C, Wang C, Zhang M, Xie Y, Schaefer HF, 3rd: Binding modes of cabazitaxel with the different human β-tubulin isotypes: DFT and MD studies. J Mol Model 2020, 26:162.

27. Duran GE, Derdau V, Weitz D, Philippe N, Blankenstein J, Atzrodt J, Sémiond D, Gianolio DA, Macé S, Sikic BI: Cabazitaxel is more active than first-generation taxanes in ABCB1(+) cell lines due to its reduced affinity for P-glycoprotein. Cancer Chemother Pharmacol 2018, 81:1095-1103.

28. Chen R, Cheng Q, Owusu-Ansah KG, Chen J, Song G, Xie H, Zhou L, Xu X, Jiang D, Zheng S: Cabazitaxel, a novel chemotherapeutic alternative for drug-resistant hepatocellular carcinoma. Am J Cancer Res 2018, 8:1297-1306.

29. Terada N, Kamoto T, Tsukino H, Mukai S, Akamatsu S, Inoue T, Ogawa O, Narita S, Habuchi T, Yamashita S, et al: The efficacy and toxicity of cabazitaxel for treatment of docetaxel-resistant prostate cancer correlating with the initial doses in Japanese patients. BMC Cancer 2019, 19:156.

30. Feng HB, Wang J, Jiang HR, Mei X, Zhao YY, Chen FR, Qu Y, Sai K, Guo CC, Yang QY, et al: β-Elemene Selectively Inhibits the Proliferation of Glioma Stem-Like Cells Through the Downregulation of Notch1. Stem Cells Transl Med 2017, 6:830-839.

31. Mu L, Wang T, Chen Y, Tang X, Yuan Y, Zhao Y: β-Elemene enhances the efficacy of gefitinib on glioblastoma multiforme cells through the inhibition of the EGFR signaling pathway. Int J Oncol 2016, 49:1427-1436.

32. Yang D, Xu X, Wang X, Feng W, Shen X, Zhang J, Liu H, Xie C, Wu Q, Miao X, et al: β-elemene promotes the senescence of glioma cells through regulating YAP-CDK6 signaling. Am J Cancer Res 2021, 11:370-388.

33. Zeng YY, Zeng YJ, Zhang NN, Li CX, Xie T, Zeng ZW: The Preparation, Determination of a Flexible Complex Liposome Co-Loaded with Cabazitaxel and β-Elemene, and Animal Pharmacodynamics on Paclitaxel-Resistant Lung Adenocarcinoma. Molecules 2019, 24:1697.

34. Cao H, Dan Z, He X, Zhang Z, Yu H, Yin Q, Li Y: Liposomes Coated with Isolated Macrophage Membrane Can Target Lung Metastasis of Breast Cancer. ACS Nano 2016, 10:7738-7748.

35. Jia Y, Sheng Z, Hu D, Yan F, Zhu M, Gao G, Wang P, Liu X, Wang X, Zheng H: Highly penetrative liposome nanomedicine generated by a biomimetic strategy for enhanced cancer chemotherapy. Biomater Sci 2018, 6:1546-1555.

36. Zhai B, Zeng Y, Zeng Z, Zhang N, Li C, Zeng Y, You Y, Wang S, Chen X, Sui X, Xie T: Drug delivery systems for elemene, its main active ingredient β-elemene, and its derivatives in cancer therapy. Int J Nanomedicine 2018, 13:6279-6296.

37. Marega R, Prasetyanto EA, Michiels C, De Cola L, Bonifazi D: Fast Targeting and Cancer Cell Uptake of Luminescent Antibody-Nanozeolite Bioconjugates. Small 2016, 12:5431-5441.

38. Zong Z, Zou J, Mao R, Ma C, Li N, Wang J, Wang X, Zhou H, Zhang L, Shi Y: M1 Macrophages Induce PD-L1 Expression in Hepatocellular Carcinoma Cells Through IL-1β Signaling. Front Immunol 2019, 10:1643.

39. Bao B, Gao D, Li N, Wu M, Xing C: Near-Infrared Light Regulation of Tumor PI3K/Akt Signaling Pathway for Enhancing Cancer Cell Apoptosis through Conjugated Polymer Nanoparticles. ACS Applied Bio Materials 2020, 3:2428-2437.

40. Gao JQ, Lv Q, Li LM, Tang XJ, Li FZ, Hu YL, Han M: Glioma targeting and blood-brain barrier penetration by dual-targeting doxorubincin liposomes. Biomaterials 2013, 34:5628-5639.

41. Shen C, Wang X, Zheng Z, Gao C, Chen X, Zhao S, Dai Z: Doxorubicin and indocyanine green loaded superparamagnetic iron oxide nanoparticles with PEGylated phospholipid coating for magnetic resonance with fluorescence imaging and chemotherapy of glioma. Int J Nanomedicine 2019, 14:101-117.

42. Yu M, Su D, Yang Y, Qin L, Hu C, Liu R, Zhou Y, Yang C, Yang X, Wang G, Gao H: D-T7 Peptide-Modified PEGylated Bilirubin Nanoparticles Loaded with Cediranib and Paclitaxel for Antiangiogenesis and Chemotherapy of Glioma. ACS Appl Mater Interfaces 2019, 11:176-186.

Figures

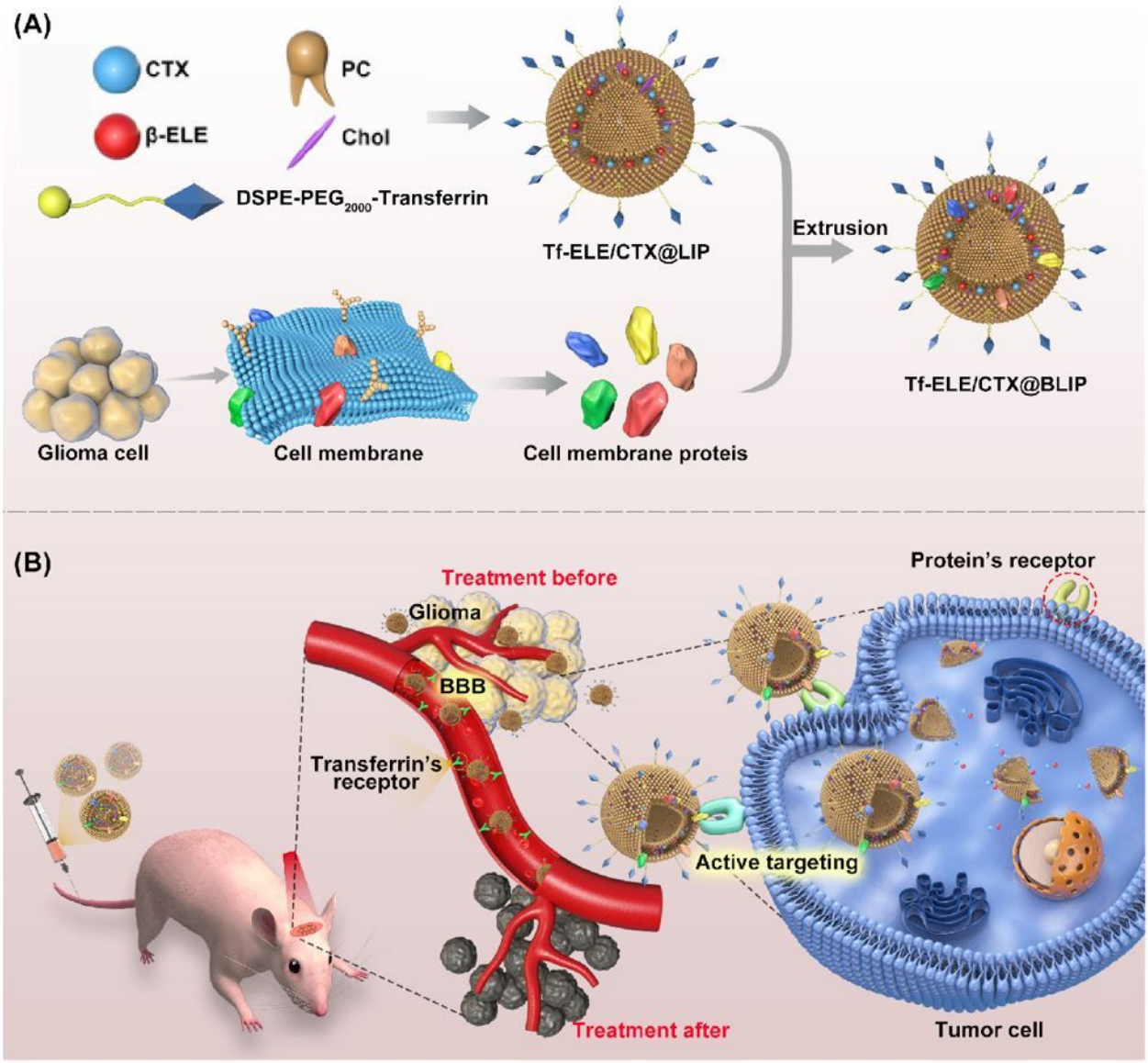

Figure 1

Schematic illustration of preparation process and active-targeting biomimetic liposomes Tf-ELE/CTX@BLIP for active-targeting penetration of BBB and homologous targeting delivery of orthotopic glioma-bearing mice. (A) Preparation approach of Tf-ELE/CTX@BLIP. (B) Schematic of Tf-ELE/CTX@BLIP for penetrating BBB and homologous targeting chemotherapy.

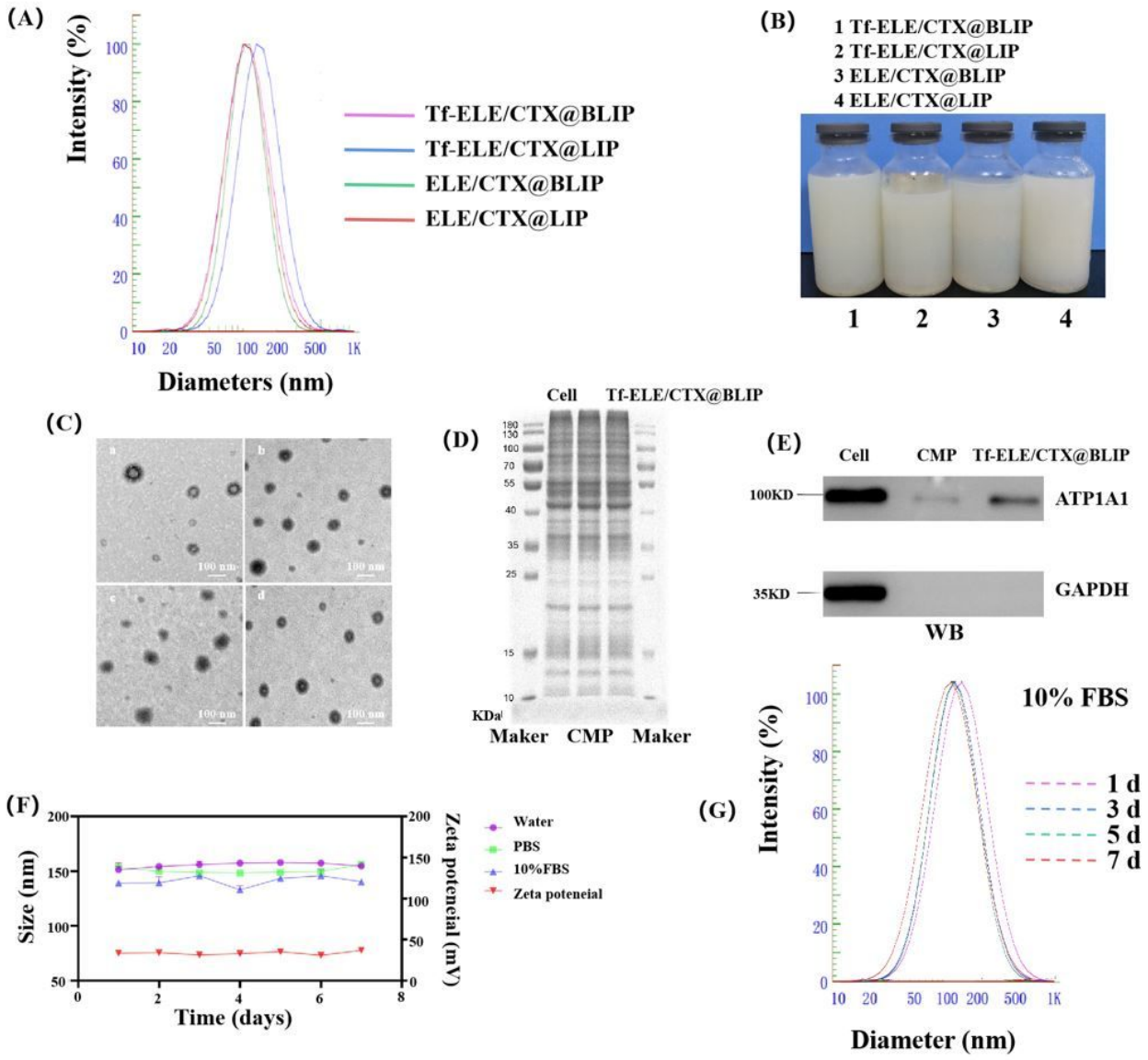

Figure 2

Characterization of biomimetic liposomes and stability evaluation. (A) Particle sizes. (B) Liposome samples. (C) TEM images of Tf-ELE/CTX@BLIP (a), Tf-ELE/CTX@LIP (b), ELE/CTX@BLIP (c) and ELE/CTX@LIP (d). (D-E) SDS-PAGE and WB analysis results of Tf-ELE/CTX@BLIP, CMP and glioma cells. (F) Hydrodynamic diameters and ζ-poteneial. (G) 7-days stability of TF-ELE /CTX@BLIP diameter in PBS containing 10% FBS.

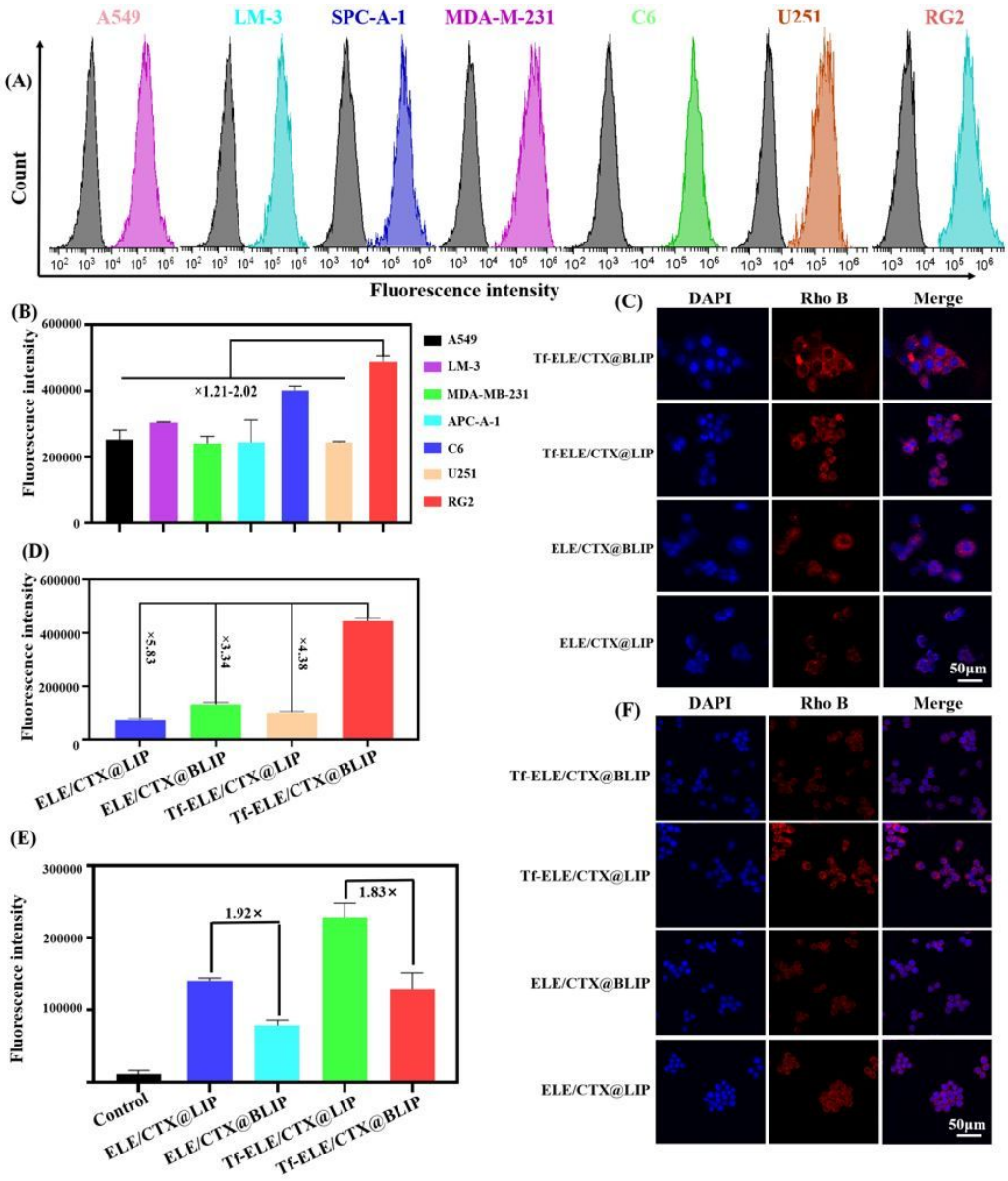

Figure 3

In vitro evaluation of immune escape and homologous targeting characteristics of Tf-ELE/CTX@BLIP. (A-B) Flow cytometry analysis and fluorescent quantitation of A549, LM-3, SPC-A-1, MDA-M-231, U251, C6 and RG2 cells treated with Tf-ELE/CTX@BLIP for 2 h. (C-D) CLSM images and fluorescent quantitation of RG2 glioma cells treated with Tf-ELE/CTX@BLIP, Tf-ELE/CTX@LIP, ELE/CTX@BLIP and ELE/CTX@LIP for 2 h. (E-F) Fluorescent quantitation and CLSM images of RAW264.7 cells after incubation with Tf-ELE/CTX@BLIP, Tf-ELE/CTX@LIP, ELE/CTX@BLIP and ELE/CTX@LIP for 2 h. Rho B = 20 μg/mL. Scale bar = 50 μm.

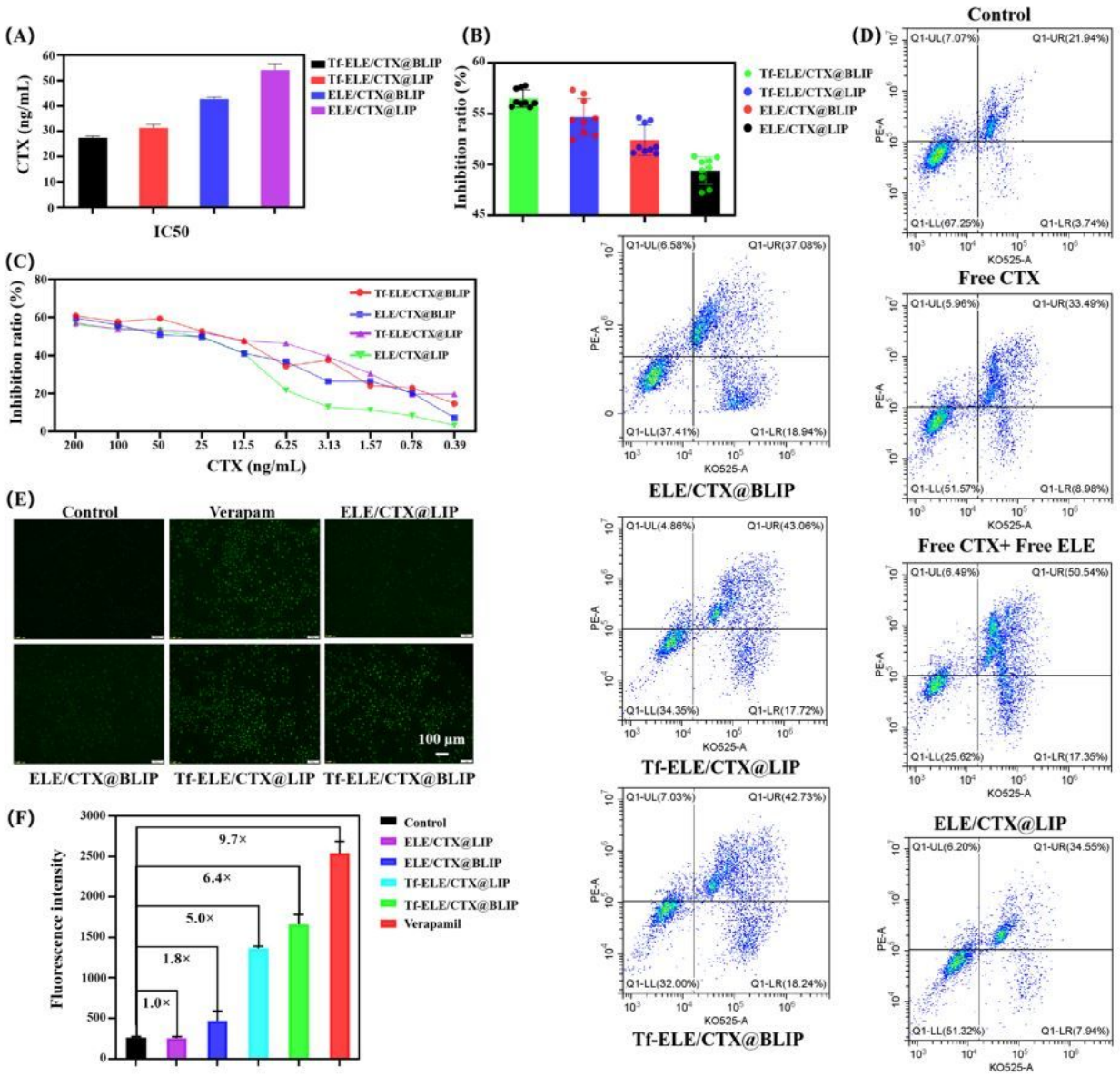

Figure 4

In vitro cytotoxicity assay and apoptosis of Tf-ELE/CTX@BLIP. (A) IC50, (B) Cell inhibition ratio (CCTX = 50 ng/mL) and (C) Cell inhibition ratio (CCTX 0.4 to 200 ng/mL) of RG2 cells treated with ELE/CTX@LIP, ELE/CTX@BLIP, Tf-ELE/CTX@LIP and Tf-ELE/CTX@BLIP for 48 h. (D) Representative results of staining and quantitative analysis of RG2 glioma cells after incubation with Tf-ELE/CTX@BLIP, Tf-ELE/CTX@LIP, ELE/CTX@BLIP and ELE/CTX@LIP for 48 h. (E) Rho 123 uptake and (F) Quantitative analysis of Rho 123 uptake by bEnd.3 cells by flow cytometry after incubation with Tf-ELE/CTX@BLIP, Tf-ELE/CTX@LIP, ELE/CTX@BLIP and ELE/CTX@LIP for 2 h. Rho 123 = 20 μg/mL. Scale bar = 100 μm.

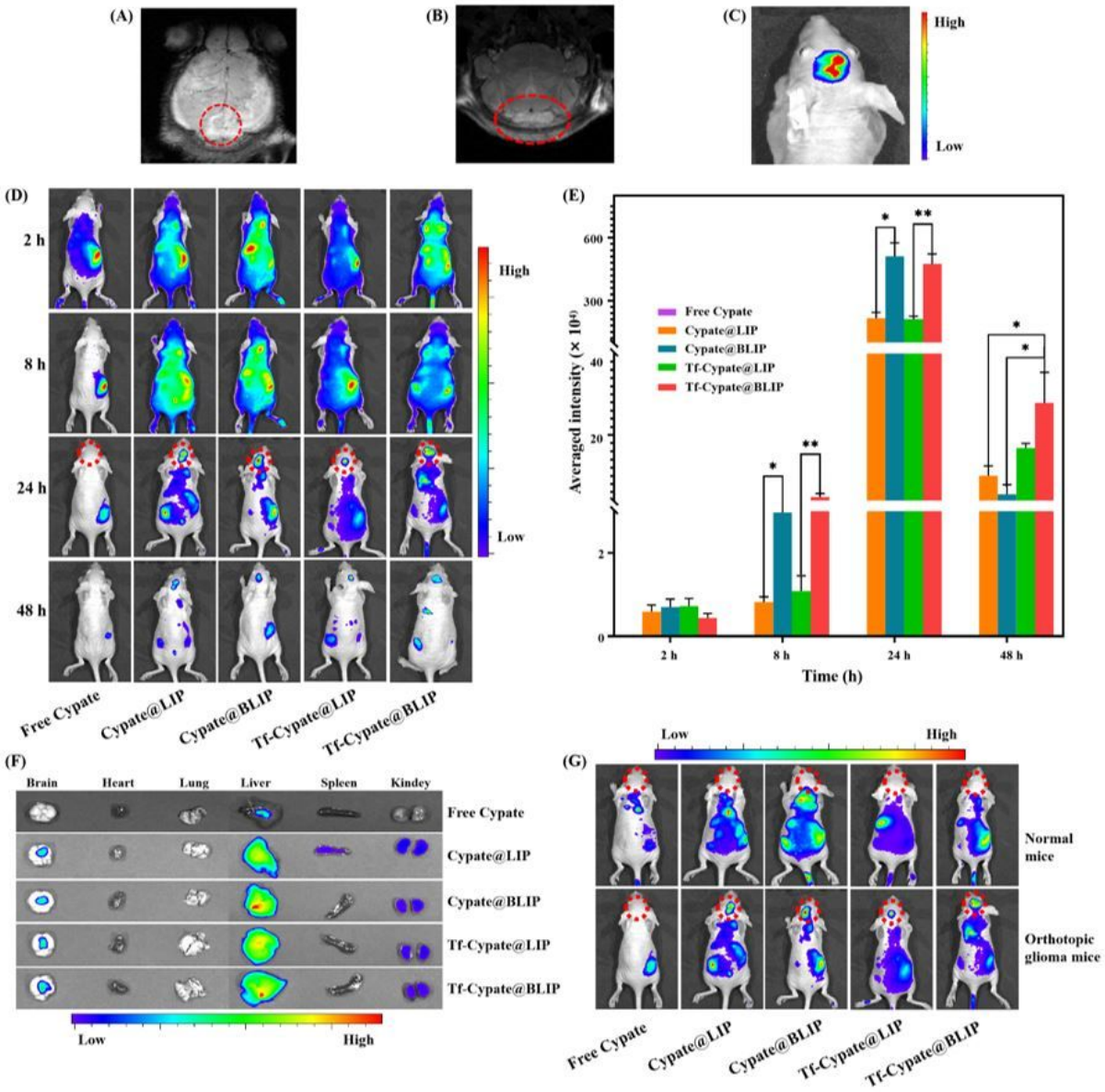

Figure 5

In vivo bioluminescence imaging of Tf-Cypate@BLIP, Tf-Cypate@LIP, Cypate@BLIP and Cypate@LIP in nude mice bearing orthotopic glioma after 15 days glioma transplantation. (A-B) Coronal and transverse cutaway view by MRI. (C) In vivo fluorescence images. (D) Bioluminescence signal distribution. (E) Bioluminescence quantitative analysis of glioma region at different times. (F) Ex vivo bioluminescence images in brains, liver, heart, spleen, lung, and kidney at 48 h post-injections. (G) Bioluminescence signal distribution in normal and orthotopic glioma mice. CCypate= 0.5 mg/kg. *p < 0.05, **p < 0.01.

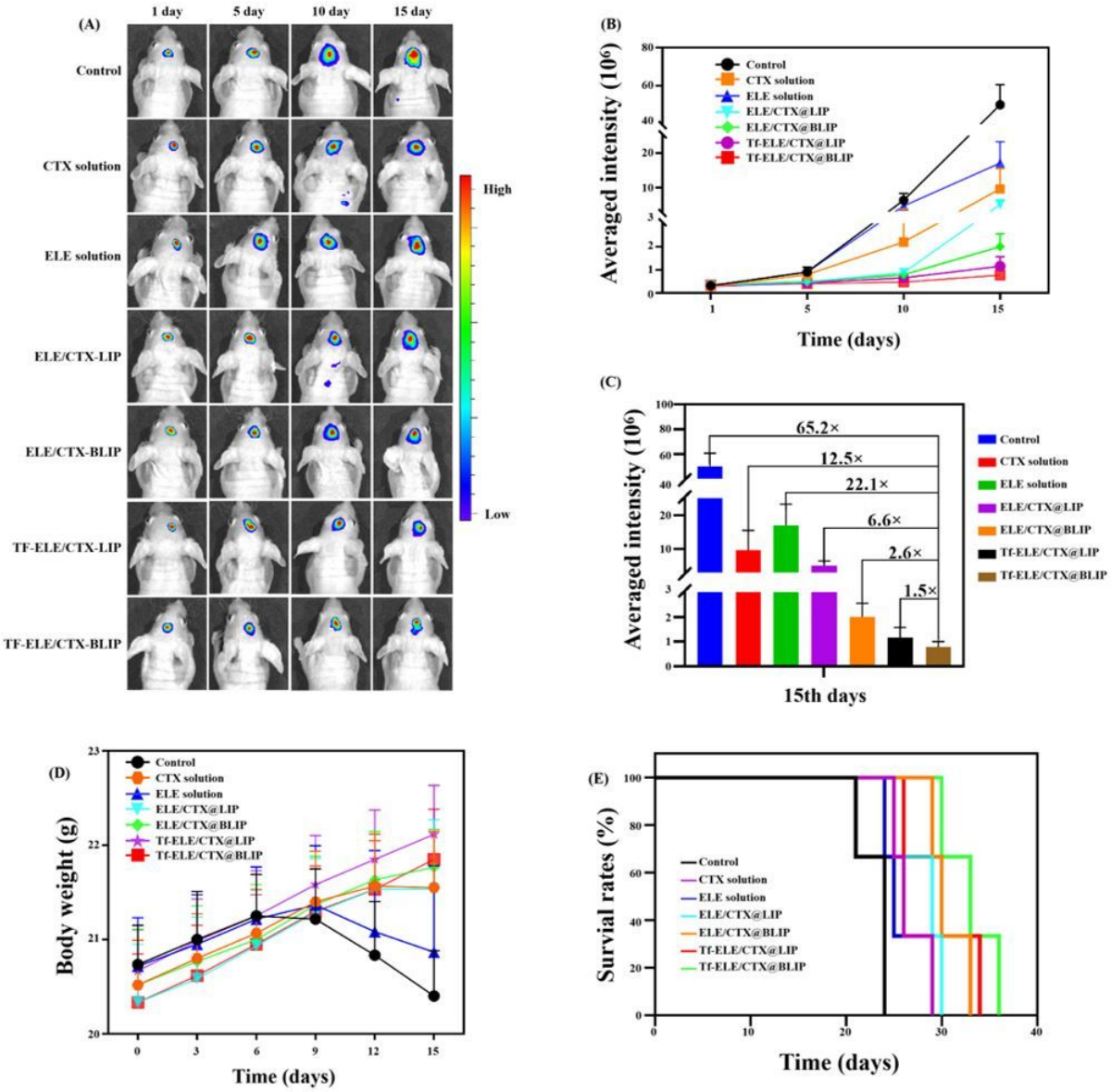

Figure 6

In vivo antitumor efficacy of Tf-ELE/CTX@BLIP in nude mice bearing orthotopic glioma. (A) Representative fluorescent images in different formulation groups. (B-C) Averaged fluorescent intensity in the brain. (D-E) Body weight and survival rate curves in different formulation groups.

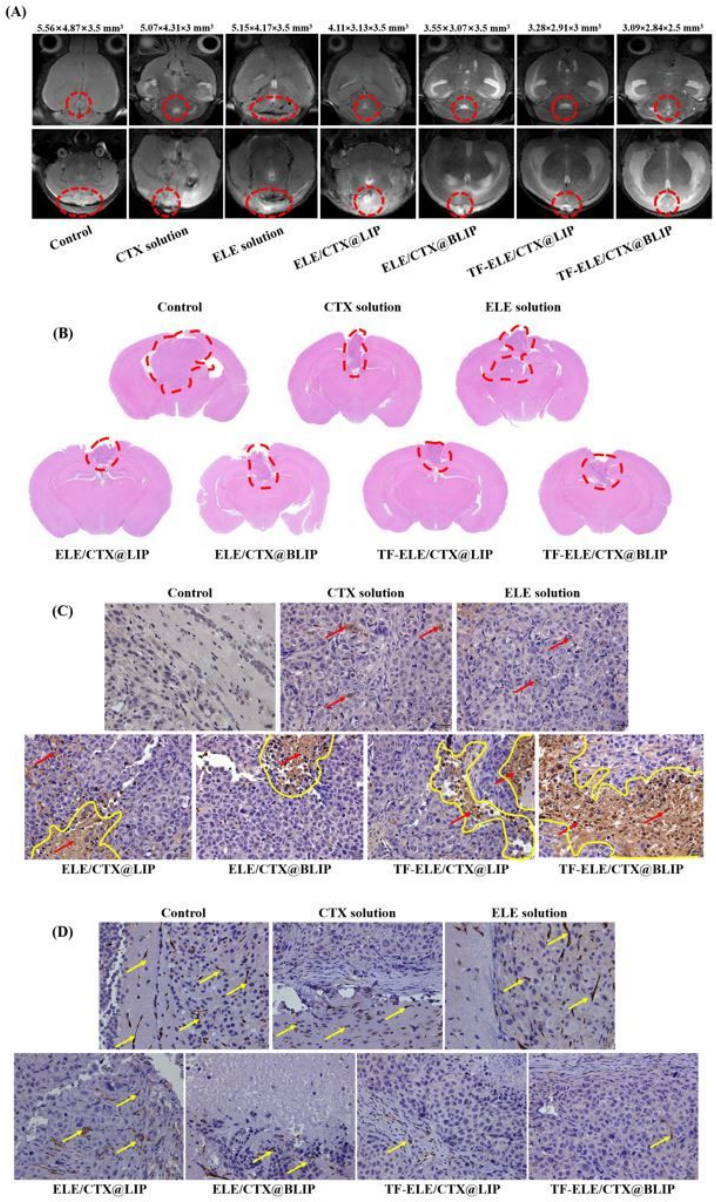

Figure 7

Anti-tumor effect of Tf-ELE/CTX@BLIP. (A) MRI observation. (B) H&E staining, ×40. (C) TUNEL analysis. Arrow: apoptosis cells, ×200. (D) P-gp expression. Arrow: the positive expression, ×200.

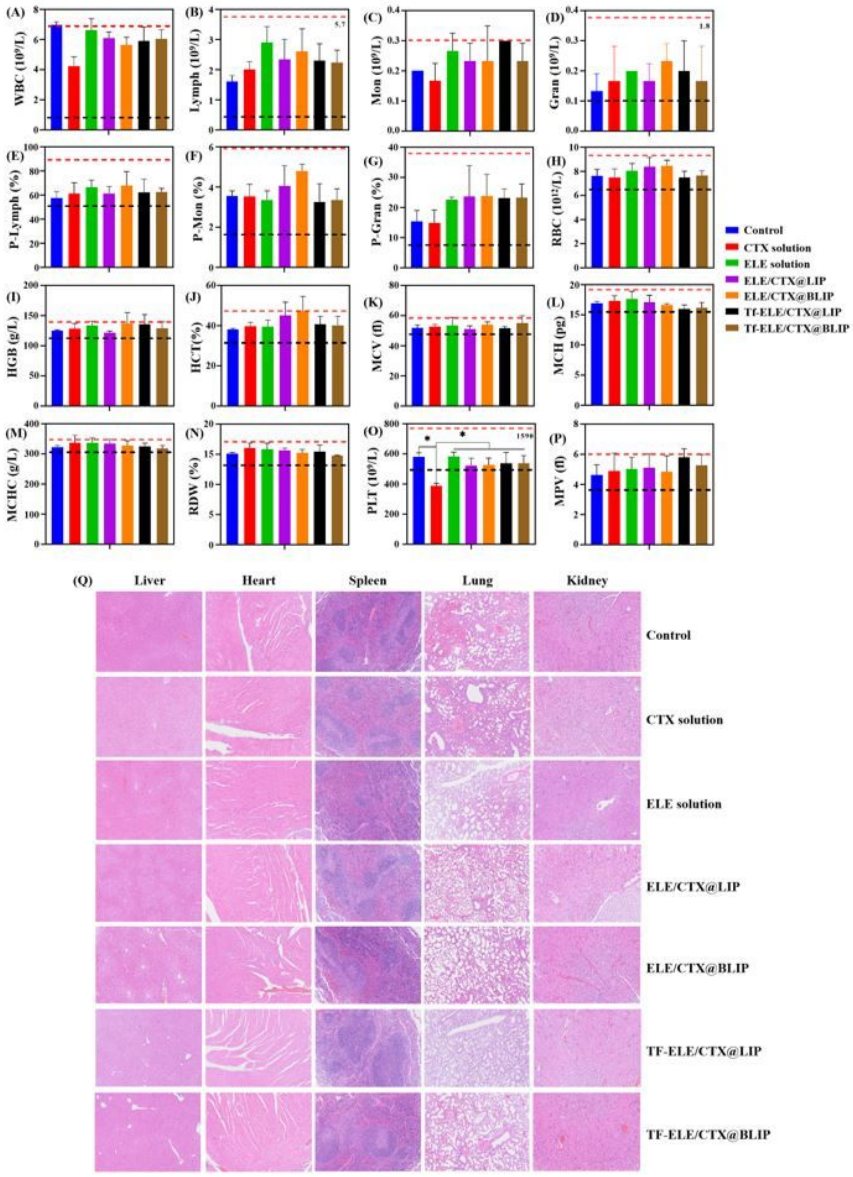

Figure 8

In vivo biosafety of Tf-ELE/CTX@BLIP. (A-P) Blood routine examination after treated with control, CTX solution, ELE solution, ELE/CTX@LIP, ELE/CTX@BLIP, Tf-ELE/CTX@LIP and Tf-ELE/CTX@BLIP. (A)WBC: white blood cell. (B) Lymph: lymphocyte. (C) Mon: monocyte. (D) Gran: neutrophil granulocyte. (E) P-Lymph: percentage of lymphocyte. (F) P-Mon: percentage of monocyte. (G) P-Gran: percentage of neutrophil granulocyte. (H) RBC: red blood cell. (I) HGB: hemoglobin. (J) HCT: hematocrit. (K) MCV: mean corpuscular volume. (L) MCH: mean corpuscular hemoglobin. (M) MCHC: mean concentration of corpuscular hemoglobin. (N) RDW: red blood cell distribution width. (O) PLT: platelet. (P) MPV: mean platelet volume. The region between black and red lines represents the normal parameter range. *$p < 0.05$, NS represents no significance. (Q) H&E staining of the major organs collected from mice sacrificed 15 days after treatment.

Supplementary Files

This is a list of supplementary files associated with this preprint. Click to download.

- Supplementarymaterials.docx